2023 IEEE International Conference on Electrical Systems for Aircraft, Railway, Ship Propulsion and Road Vehicles & International Transportation Electrification Conference (ESARS-ITEC) | 979-8-3503-4689-3/23/$31.00 ©2023 IEEE | DOI: 10.1109/ESARS-ITEC57127.2023.10114820

Ground-based power supply system to operate hybrid-electric aircraft for future regional airports

Markus Meindl
Institute for Power Electronics
Friedrich-Alexander-Universität
Erlangen-Nürnberg (FAU)
Nuremberg, Germany
markus.meindl@fau.de

Martin März
Institute for Power Electronics
Friedrich-Alexander-Universität
Erlangen-Nürnberg (FAU)
Nuremberg, Germany
martin.maerz@fau.de

Kai Johannes Weber
Institute for Power Electronics
Friedrich-Alexander-Universität
Erlangen-Nürnberg (FAU)
Nuremberg, Germany
kai.johannes.weber@t-online.de

***Abstract* — Transforming air traffic from fossil fuels to sustainable air traffic poses new challenges for airports. The charging infrastructure and aircraft fueling at future airports must also adapt to sustainable, electric aviation. This paper presents a MATLAB Simulink model of a future airport using data from a regional airport. This model simulates the initial estimates for an airport's entry into a sustainable aviation industry. Based on a flight plan of the regional airport, the aim is to determine which service levels are required and which options are available for future scenarios. For this purpose, a charging profile for aircraft batteries was created to meet the challenges of short ground times for regional aircraft. The model analyses suitable supply technologies for energy storage on the ground, grid connection and energy transmission to the aircraft.**

Keywords—hybrid-electric aircraft, power supply, fast-charging, power transfer

I. Introduction

The project "Gauging the ENvironmEntal Sustainability of electrIc aircraft Systems" (GENISIS) is an EU funded project to develop a technology and sustainability roadmap. This roadmap shall help to support the ambitions of the European aviation industry for transitioning towards environmentally sustainable and competitive electric and hybrid aircraft systems. The project's period from 2025-2055 considers different time horizons and scenarios [1]. Rotterdam The Hague Innovation Airport (RTHA) is a partner of GENISIS and seeks to change its infrastructure to adapt to the transition of aircraft types. To accomplish this, RTHA plans to electorate its aircraft movements of around 70% from the year 2030 onwards and aims to replace the remaining 30% with hydrogen-powered aircraft by the year 2050 [2]. Furthermore, aircraft manufacturers like Airbus plan to introduce hydrogen aircrafts by 2035. With the code ZEROe (short for zero emissions), Airbus is planning three types of passenger planes that will rely on liquid hydrogen as fuel [3]. Surplus energy from photovoltaics could produce emission-free hydrogen (green hydrogen). The aim was to create a basic simulation model for an airport of the future. Above all, considers the increasing energy consumption of electrical energy due to the electrification of aircraft movements. Data from RTHA and other project partners will be used for this purpose. In addition, the aim is to improve the system's energy efficiency with a battery model and to test the concept of a large electrolyzer to gain information about on-site hydrogen production. Further investigations will be carried out on more detailed models of the PV park and the electrolyzer.

II. Simulation Model - Background

RTHA delivered a measured annual energy requirement of 6 GWh for their residential load and a history of the active power consumed over a good day. In addition, a flight plan with a total of 25 departures to 18 destinations was shared [2]. The planned aircraft in GENISIS is a hydrogen hybrid aircraft with additional batteries. The maximum flight range of the GENISIS aircraft is 1500 km, and the maximum number of passengers (PAX) is 50. Because of the limited capacity, only half of the destinations can be replaced by GENISIS aircraft, reducing the number of departures to be electrified on this day to 14. According to the flight information, the number of passengers on almost all flights is more than 50, meaning that these flight connections must be replaced with more than one GENISIS aircraft, as seen in Table I.

TABLE I DEPARTURES FORM RTHA THAT CAN BE REPLACED BY GENESIS AIRCRAFTS ON EXEMPLARY DAY

Flight number	Departure	Destination	Distance in *km*	PAX	Amount GENISIS airplanes
1	7h01	GRO	1125	185	4
2	7h08	SPU	1286	175	4
3	7h12	MPL	932	178	4
4	7h14	LCY	305	37	1
5	7h28	PSA	1020	169	4
6	7h28	PSA	1020	169	4
7	7h41	PMI	1385	186	4
8	10h16	LCY	305	71	2
9	11h55	IBZ	1474	185	4
10	12h04	PUY	1050	176	4
11	12h55	GRO	1125	180	4
12	12h59	DBV	1472	159	4
13	13h05	PMI	1385	176	4
14	15h43	LCY	305	69	2

This replacement leads to 49 GENISIS aircraft that must charge within this exemplary day. According to our partners at Bern University of Applied Sciences, for the GENISIS aircraft, there are two batteries with a capacity of 410 kWh necessary [4]. To reduce the charging time of the batteries from 1 h to 45 min a C-rate of 1.5 was chosen which leads to a charging power of 615 kW and consequently 1230 kW for each aircraft. Under the assumption, that a busy day with 49 airplanes to charge per day can be applied to a whole year, the annual energy consumption of the charging stations results in 16.51 GWh as seen in (1)

$$E_{charge} = 365.25 \cdot 49 \cdot 0.75\ \text{h} \cdot 1230\ \text{kW} = 16.51\ \text{GWh} \quad (1)$$

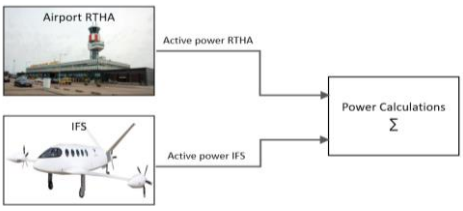

Fig. 1. Structure of simulation model with airport and IFS

Together with the annual airport's energy requirement of 6 GWh, this results in energy consumption of 22.51 GWh per year. The RTHA's planned PV system with an annual yield of 13.6 GWh will not be able to cover the airport's needs. It should be noted, however, that the energy production of a PV system differs seasonally and therefore in months with the highest solar radiation there is a chance of oversupplying the grid with photovoltaics. First, in MATLAB/Simulink, a simple model was created to verify the results already obtained. In addition, a MATLAB parameter file was created containing important parameters, profile data, and a MATLAB function explained in this chapter. To simulate the annually measured energy consumption of the airport, the course of the consumed active power of an exemplary day was implemented with a lookup table. The lookup table is located in the Airport RTHA block, and the resulting data with the simulation time of one day is fed into the power calculation block, as shown Fig. 1. This data were also assumed to be the same for every day in the year to perform a rough calculation of the annual consumed power by the residential load. Therefore, the active power of the airport is summed up, converted from watt seconds (Ws) to watt hours (Wh) and then multiplied with a gain of 365.25 in the power calculations subsystem. The resulting value was considerably higher than the measured value of 6 GWh. To match with the measured value the received data needed to be lowered by 0.32 MW at every time of the day which is shown in Fig. 2.

For the simulation of the IFS's switching signals which determine the charge cycles of the aircrafts are implemented as look up tables in the IFS block. The logic signal itself is generated by a function written in Matlab. The input signals of this function are a simulation time in minutes, a charge time in minutes, a buffer time in minutes (the time between two charges) and further a start and end time given in 24 h format. Beginning from the start time, logic ones will be generated into the timetable for the period of one charge which is directly followed by logic zeros for the period one buffer time. This will be repeated until the end time which results a timetable with Boolean values in a pulse width modulated manner. Considering the high number of aircraft that need to charge, the number of chargers is selected to be four. This selection helps divide up the aircraft's charges during periods of the day that resemble the flight plan to some extent. For a charging time of 45 min, all chargers are selected to have buffer times of 15 min. Therefore, a charge and replacement of an aircraft at one charger occupy precisely one hour. The switching signals from chargers 1 to 3 are scheduled from 6 a.m. to 6 p.m., each charging 12 jets daily. The passed switching signals multiplied in Simulink with a charging power of 1230 kW, representing the charging power of one GENISIS aircraft. The sum of the active power trends of the four ideal fast-charging Stations (IFS) can observe in Fig. 1. Like the airport's load, the charging stations' active power is also summed up, converted, and multiplied with a gain of 365.25 to obtain a rough annual energy. This helps to divide up the charges of the aircrafts during periods of the day that resemble the flight plan in Table 1 to some extent. For a charging time of 45 min all chargers are selected to have buffer times of 15 min. Therefore, a charge and replacement of an aircraft at one charger occupies exactly one hour. The switching signals from charger 1 to 3 are scheduled from 6 a.m. to 6 p.m., each charging 12 aircrafts during the day. Charger 4 charges an hour longer and thus charges a total of 13 aircrafts, which results with the other chargers to a total of 49 aircrafts that are charged during the day. The passed switching signals are multiplied in Simulink with a charging power of 1230 kW representing the charging power of one GENISIS aircraft. Like for the residential load of the airport, the active power of the charging stations also is summed up, converted from Ws to Wh and then multiplied with a gain of 365.25 to obtain a rough annual energy consumption. By summing up the adjusted power trend of the airport from Fig. 2 the simulation delivers a total annual power consumption of 22.55 GWh which almost matches with the value from the rough calculation.

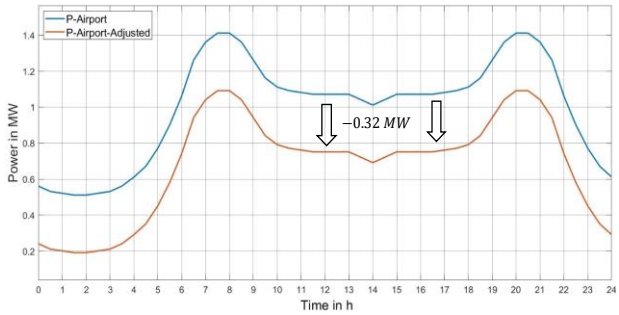

Fig. 2. Actual and adjusted active power trend of airport

III. Expansion of the Simulation Model

To investigate the potential oversupply of the PV and the impact of energy storage systems, simplified models of a PV farm, a battery and an electrolyzer were added to the model structure as can be seen in Fig. 3

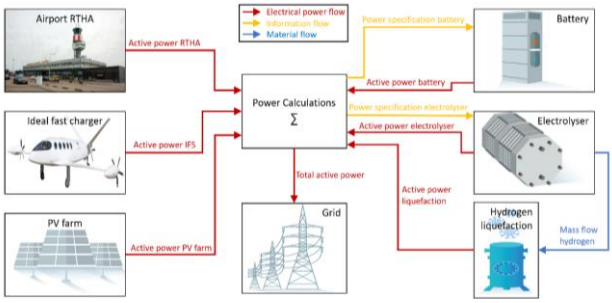

Fig. 3. Expanded structure of the simulation model

A. PV farm model

For the implementation of a PV farm model, RTHA supplied data of the global horizontal irradiance (GHI) for the year 2021 for every 5 minutes. According to [5] the solar energy output of a PV system can be calculated with the formula seen in (2) which was also verified with the text book "Photovoltaik Engineering" by Andreas Wagner [6]

$$E_{PV} = A \cdot r \cdot H \cdot PR \tag{2}$$

The variable A stands for the total solar panel area in square meter (m^2), the solar panel yield is represented by the variable r in percent (%), H is the solar radiation on tilted panels within a given time in watt-hours per square meter (Wh/m^2) and PR is the performance ratio. The solar panel yield is given by the electrical power in Watt-peak (Wp) divided by the area of one panel and the standard test conditions (STC) of radiation with 1000 W/m^2 at a cell temperature of 25 degree Celsius (°C), a wind speed of 1 meter per second (m/s) and an air mass of 1.5. As an example, and as value for the PV farm model, the solar panel yield of a PV module of 250 Wp with an area of 1.6 m^2 calculates to

$$r = \frac{250\ \mathrm{Wp}}{1.6\ \mathrm{m}^2 \cdot 1000\ \frac{\mathrm{W}}{\mathrm{m}^2}} \cdot 100\% = 15.63\ \% \tag{3}$$

While in [5, 6] the solar radiation is specified as an average value over an period, for the simulation in Simulink this value is being calculated with radiation data on a five-minute interval basis over a specified simulation time which lasts up to a whole year. It is also important to note that the GHI value was used as radiation value. In the future and with consultation of RTHA the global tilted irradiance (GTI) can be modelled from the GHI with knowledge of the specific inclination and orientation of the PV panels.The performance ratio is ranging between 0.5 and 0.9 and includes the losses of the PV installation. According to [5] the two biggest contributors for the PR are the temperature and shadings losses. For this level of consideration, the PR value will be assumed to be constant at 0.75. For the simulation model the GHI data is implemented as a lookup table in the PV farm block and the output being multiplied with the value of r and PR chosen as reasoned above. The structure of the PV farm block is visible in Fig. 4. The area of the solar panel is chosen to be 1100 m^2 to match the result of a one-year simulation in Simulink with the annual yield of 13.6 GWh that is planned by RTHA. In order to cope with a whole year simulation, the calculation time of the simulation is minimized by increasing the fixed-step size of the solver to 300 seconds (sec) to match with the 5-min interval of the irradiation data. At this point it is important to note that the increase of the fixed-step size has an impact on the active power trend of the IFS, because their switching signals are based on a one-minute interval. It can be observed that the duration of the switch between the charging power and zero in the active power trend lags by exactly 300 sec reducing the buffer time from 15 min down to 10 min. Nevertheless, the annual power consumed of the fast-charging stations stays accounting wise the same, as long the fixed-step size of the solver is not increased more than the buffer time of the IFS itself. Since the lookup table of the residential load of the airport and the IFS are designed for only a one-day simulation, a control logic to reset the time after one day must be implemented in their subsystems to enable a repeating sequence for those trends. The control logic capable of doing this uses a sample-based pulse generator with a period that results from the seconds of a day divided by the sample time of 300 sec. To investigate the potential oversupply of the PV farm, the active power trend from the airport and the fast-charging stations are given a minus sign and are then summed up with the active power trend.

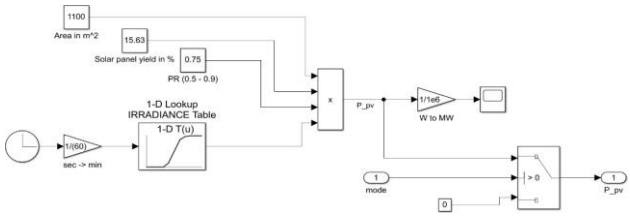

Fig. 4. Structure of PV farm block

B. Battery model

To in case of an over-supply or demand of power it can be helpful to introduce a battery system into the model to obtain a balancing factor with quick reaction time. The battery model shall aim to reduce the area below zero and therefore reduce the consumption of network power. Due to time constraints, it was not possible to conduct profound research on the battery technologies that might be at the advance in the next decades and probably the best choice concerning a power grid of an airport in the future. Therefore, the battery model from the project Microgrid-EMS-Optimization [7] was used since it uses a simplified modelling method for a battery system. The model was modified in a manner that it uses a spectrum of a charge and discharge rate for the battery and calculates with progressing time the state of charge (SOC) of the battery considering an efficiency of the battery as can be seen in Fig. 7. Further, the model has constraints concerning the upper and lower charging level of the SOC which can be observed with the other parameters in Table II. The data which is responsible for the power specification of the battery is defined as "P_spec_batt" and originates from the sum of the PV farm, the IFS and the airport as seen in (4). The battery block „P_{spec_batt}" is limited according to the

maximum charge and discharge rate of the battery which is passed as "P_in" into the SOC calculation block. Further, the SOC calculation block has a feedback loop about the SOC of the battery. The implemented control logic in the SOC calculation block is straight forward. If "P_in" has a positive sign and the SOC is below the upper charging limit, this specifies the state of charging for the battery. In the other case if "P_in" has a negative sign and the SOC is higher than the lower charging limit, this specifies the state of discharging for the battery. For the charging operation the efficiency of 0.96 is applied whereas for the discharging the reciprocal is used. This has the effect that the charging process will take longer than the discharging for the same SOC change. The responsible logic signal for an exemplary period (end of May) without the effect of the IFS.

TABLE II. BATTERY PARAMETERS ADOPTED FROM [7]

Battery capacity	Max. charge rate	Max discharge rate	Upper charging level of SOC	Lower charging level of SOC	Efficiency
2.5 MWh	400 kW	-400 kW	85%	19%	0.96

$$P_{spec\_batt} = P_{PV} + P_{IFS} + P_{airport} \tag{4}$$

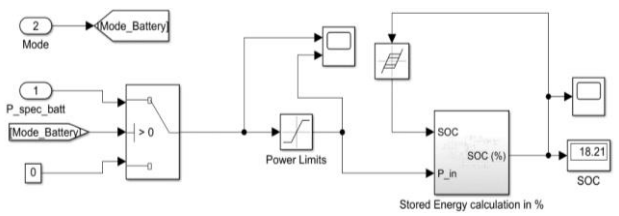

Fig. 5. Structure of the battery block

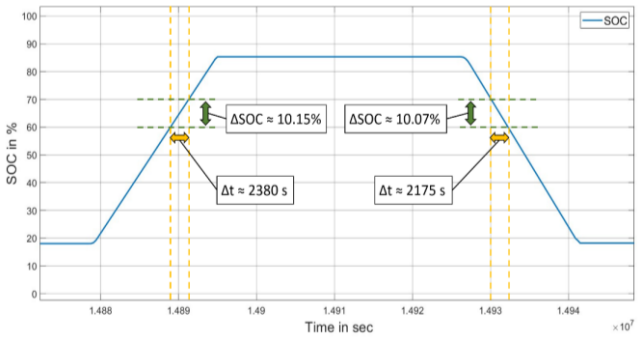

Fig. 6. SOC of the battery during a period at the end of May

A positive 1 corresponds to a discharging action, a negative 1 to a charging action and a zero to no battery action. The logic signal can be verified with the slopes of the SOC in Fig. 6 where a falling slope corresponds to a discharging action and a rising slope to a charging action. Additionally, the correct implementation of the efficiency can be verified by calculating the necessary time for a change and discharge rate is calculated in (5) and (6) and match with Fig. 6. Whenever there is a battery action, P_{in} is channelled back to the power calculations block with a switched sign as the active power of the battery "P_batt". There, P_{batt} gets summed up with P_{spec_batt} to the power specification of the electrolyzer "P_spec_elec" as can be seen in (7). The data of P_{spec_elec} is needed for the operation of the electrolyzer which will be discussed in the next chapter.

$$\Delta t_{charge} = \frac{\Delta SOC \cdot E_{batt}}{P_{max} \cdot \eta_{charge}} \approx 2379 \text{ sec} \tag{5}$$

$$\Delta t_{discharge} = \frac{\Delta SOC \cdot E_{batt}}{P_{max} \cdot \frac{1}{\eta_{charge}}} \approx 2175 \text{ sec} \tag{6}$$

$$P_{spec\_elec} = P_{spec\_batt} + P_{batt} \tag{7}$$

The effect of the battery during the already looked upon period is visible when P_{spec_batt} and P_{spec_elec} are plotted together as seen in Fig. 7. The battery shows the desired effect of reducing the area below zero for the plot of P_{spec_batt} by the expanse of the area above zero. If P_{spec_batt} is within the range of the maximum charge and discharge rate of the battery, which is visible as the area between the yellow lines in Fig. 8, the battery can keep the total active power at zero. Since the battery has no maximum charge and discharge rate during those periods, the slope is not at its maximum and depends on the current value of P_{spec_batt} within these boundaries. Above and below the yellow lines the battery is working at maximum charge and discharge rate provided the SOC is not at its upper or lower charging limit. The battery system shows promising results but for the future after the selection of a suitable battery technology a more detailed model should be implemented which considers things such as performance factors e.g. temperature, SOC, charge current, etc. but also degradation factors such as calendar or cyclic degradation.

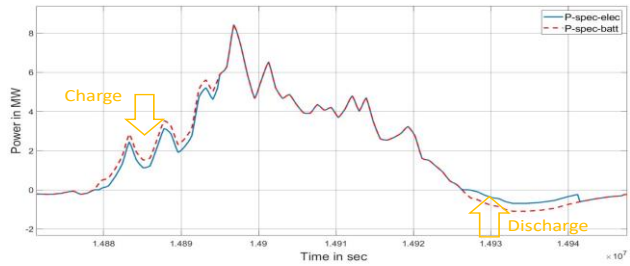

Fig. 7. Trends of P_{spec_batt} and P_{spec_elec} during end of May

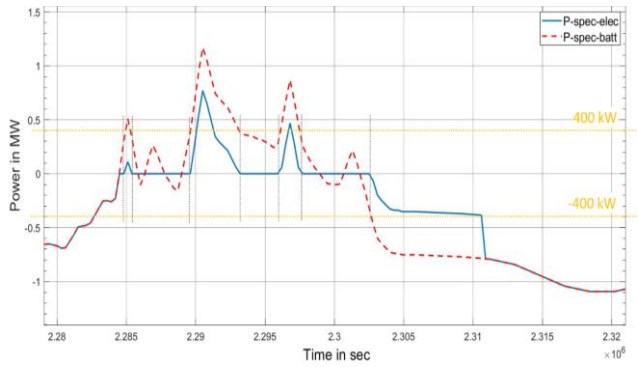

Fig. 8. Trends of P_{spec_batt} and P_{spec_elec} during end of January

C. Electrolyzer Model

For the Simulink model a simplistic model for a big electrolyzer was found in a way that it is based on an empiric model of a 6 MW electrolyzer located in Energiepark Mainz. The hydrogen production and efficiency as a function of the total power consumption of the power to gas (PtG). The efficiency plot includes the total power consumption of all the ancillary components such as transformers, rectifiers, ionic compressor, pumps, cooling units and infrastructure at an output pressure of 22.5 megapascals (MPa). The efficiency plot was reproduced in excel to use the data in a lookup table in the electrolyzer block as seen Fig. 9. The necessary formula to calculate the produced hydrogen originates from [8, 9][9] and is defined as (8), which is implemented in the hydrogen production block, expresses the flow of amount of hydrogen substance ($\dot{n}_{H2}$) produced depending on the overall efficiency (η_{HHV}), the higher heating value (HHV), and the electric power (P_{el_elec}) that is applied.

$$\dot{n}_{H2} = \frac{P_{H2}}{HHV} = \frac{\eta_{HHV} \cdot P_{el\_elec}}{HHV} \tag{8}$$

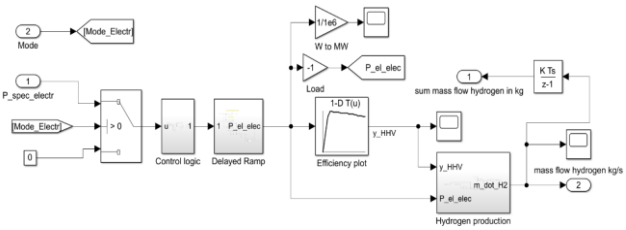

Fig. 9. Structure of electrolyzer block

Additionally, a conversion from $\dot{n}_{H2}$ to a mass flow of hydrogen ($\dot{m}_{H2}$) with the molar mass of hydrogen is conducted whose result is then summed up and displayed but also channelled out to the liquefication block as shown in Fig. 3. In the electrolyser block the electric power is specified as a ramp function with a certain end value in the delayed ramp block. The end value of the ramp function will determine the power operating point of the plant and the slope will define how fast this point will be reached. In terms of when the electric power will be applied certain criteria were defined in the control logic block. These criteria are on the one hand that the battery performs no charging or discharging action ($P_{batt} = 0$) and on the other hand that at least half of the required power of the power operating point (P_{op_elec}) is available ($P_{spec\_elec} > P_{op\_elec}/2$). The latter was formulated to prevent significant distortions in the total power trend which results from the used electric power of the plant. An exemplary ramp function of the electric power with $P_{op\_elec} = 4$ MW but without the effect of the IFS.

D. Hydrogen Liquefication model

The liquefication of hydrogen is highly complex but also highly power demanding. Regarding the level of consideration of the model this process is included with a characteristic value of power consumption to convert one kilo of gaseous hydrogen into liquid form. The mass flow of hydrogen from the electrolyzer block is channelled into the liquefication block where it is multiplied with characteristic value of 12 kilowatt hours per kilograms (kWh/kg) hydrogen that was found in [10]. It is important to note that the literature refers to the liquefication of hydrogen at ambient temperature and pressure whereas the produced hydrogen from the electrolyzer model is pressurized at 22.5 MPa. Therefore, the characteristic value of liquefication may be lower. The additional power of liquefaction (P_{liq}) is added on top of the electric power consumed by the electrolyzer, which is added up with the power specification of the electrolyzer to the total active power in the power calculation block:

$$P_{total} = P_{spec\_elec} + P_{el\_elec} + P_{liq} \tag{9}$$

On first sight the activation of the electrolyzer seems to be delayed because the electrolyzer should be activated when P_{spec_elec} reaches half of the value of the power operating point which is 2 MW. Nevertheless, when P_{spec_elec} falls below 2 MW again at around $1.3888 \cdot 10^7$sec the electrolyzer is shut off as planned. This supposedly inconsistency can be discarded when the composition of the logic signal responsible for activating the electrolyser. Since the logic signal of the electrolyzer is bound to an AND condition, the logic signal of the electrolyzer is delayed by the battery which is activated until around $1.3854 \cdot 10^7$sec.

E. Grid Model

The total active power of the system as described in (9) is channelled as the result of the power calculation block into the grid block as seen in Fig. 3. The grid block in its basic function filters out the positive value of "P_total" and thereby tracks the power lack during the year. The negative value of "P_total" gets summed up and delivers an energy value at the end of the simulation which needs to be supplied by the grid. The structure of the grid block is thereby simplistic as seen in Fig. 10. The liquefication of hydrogen is highly complex but also highly power demanding.

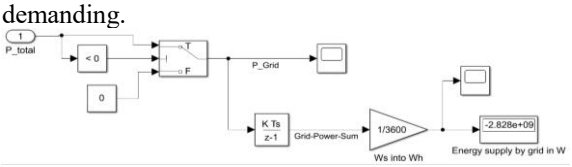

Fig. 10. Structure of grid block

IV. Simulation Results

While the previous sections were focused on the construction of the system components and their verifications in terms of functionality, this chapter gives simulation results with absolute numbers regarding the impact of system components on the active power that needs to be provided by the grid but also the hydrogen that is produced. To simplify the simulation results different scenarios of active and inactive system components were constructed with Table III. The first four scenarios include only the airport as an active load and per scenario the energy

source as PV and energy storages as the battery and the electrolyzer are added. The last four scenarios follow the same principle with the difference that the active loads are the airport and the IFS. A cross represents an inactive component, and a check mark stands for an active component. The results on the energy that needs to be supplied by the grid and the produced hydrogen over the period of one year for the different scenarios can be observed in Table IV.

Table III. Active and inactive system components

Scenario	Airport	IFS	PV	Battery	Electrolyzer
1	✓	×	×	×	×
2	✓	×	✓	×	×
3	✓	×	✓	✓	×
4	✓	×	✓	✓	✓
5	✓	✓	×	×	×
6	✓	✓	✓	×	×
7	✓	✓	✓	✓	×
8	✓	✓	✓	✓	✓

Table IV. Results for different scenarios

Scenario	Energy supplied by grid in GWh	Hydrogen produced in tons
1	6.03	0
2	2.96	0
3	2.42	0
4	2.83	32.69
5	22.53	0
6	12.88	0
7	12.47	0
8	12.52	3.74

The first thing that is interesting to note is that the impact of adding PV power to the loads cuts the energy that needs to be supplied by the grid by half if no IFS are applied. However, if the IFS are applied the PV farm is only capable to reduce the energy that needs to be covered by the grid by 43%. This implies that during active phases of PV power the power necessary for the IFS cannot be covered fully by the PV farm. By adding the battery system, the amount of energy that is saved is 0.54 GWh from scenario 2 to 3 and 0.41 GWh from scenario 6 to 7. This concludes that the effect of the IFS have a mitigating effect on the effectiveness of the battery. For the two scenarios that the electrolyzer is also active it can be observed that the production of hydrogen is 8.74 times higher if the IFS are not active. The extra energy that is necessary from scenario 3 to 4 is 0.41 GWh and from scenario 7 to 8 only 0.05 GWh. Although it can be said that the effect of the IFS reduces the hydrogen production significantly, a profound investigation to what extend the extra energy is responsible for the difference of produced hydrogen for those two changes of scenarios needs to be conducted in the future.

V. Conclusion

In this paper, a Matlab-Simulink simulation model for future regional airports is introduced, which gives an outlook for the high-power demand of electricity, and liquid hydrogen needed to supply hybrid-electric aircraft. The question about how high the annual energy requirement of the airport is to be estimated by the RTHA due to the Addition of partial electrification of the aircraft movements. It was found that RTHAs planned PV farm would not be able to cover the airport's needs. Based on a daily active power consumption trend of the airport and a self-created trend for the IFS, the result of the investigation is recreated in Simulink. For future estimations, further system components were added: a PV farm model, a battery model, and an electrolyzer model. The PV farm model as an energy source was implemented into the energy model with a simple equation describing a PV system's solar energy output. The Addition of the loads and the source led to a power trend used by the battery. The battery model was implemented in a way that reduces the lack of energy throughout the year by the expanse of excessive energy that roots from the PV farm. Due to the capacity limitations of the battery and the potential need for hydrogen for hydrogen-based aircraft, an empirical model of a 6 MW electrolyzer was constructed. For the future, the energy model shall be extended in a manner of deeper considerations to dispose of the disadvantages of the model, which originate from its simplifications at its current status.

VI. References

[1] Dr. Alexis Laurent, *GENESIS-The Project.* [Online]. Available: https://www.genesis-cleansky.eu/ (accessed: Aug. 2 2022).

[2] Cor de Ruiter, *Infrastructure Airport Rotterdam*.

[3] Airbus, *ZEROe-Towards the world's first zero-emission commercial aircraft.* [Online]. Available: https://www.airbus.com/en/innovation/zero-emission/hydrogen/zeroe (accessed: Aug. 2 2022).

[4] Bruno Lemoine, *Batteries in GENESIS aircrafts*.

[5] Photovoltaic-software.com, *How to calculate the annual solar energy output of a photovoltaic system?* [Online]. Available: https://photovoltaic-software.com/principle-ressources/how-calculate-solar-energy-power-pv-systems (accessed: Aug. 2 2022).

[6] A. Wagner, Ed., *Photovoltaik Engineering. Berlin*. Berlin Heidelberg: Springer, 2019.

[7] J. LeSage, *Microgrid Energy Management System (EMS) Using Optimization.* [Online]. Available: https://github.com/jonlesage/Microgrid-EMS-Optimization (accessed: Dec. 4 2022).

[8] J. Töpler and J. Lehmann, *Wasserstoff und Brennstoffzelle*. Berlin, Heidelberg: Springer Berlin Heidelberg, 2017.

[9] J. Töpler und J.Lehmann, Ed., *Wasserstoff und Brennstoffzelle*. Berlin, Heidelberg: Springer Berling Heidelberg, 2017.

[10] M. C. Möller and S. Krauter, "Hybrid Energy System Model in Matlab/Simulink Based on Solar Energy, Lithium-Ion Battery and Hydrogen," *Energies*, vol. 15, no. 6, p. 2201, 2022, doi: 10.3390/en15062201.